Inclusive Electron-Nucleus Scattering at Large Momentum Transfer

J. Arrington,[2,*] C. S. Armstrong,[11,†] T. Averett,[2,‡] O. K. Baker,[4,9] L. de Bever,[1] C. W. Bochna,[5] W. Boeglin,[3] B. Bray,[2] R. D. Carlini,[9] G. Collins,[6] C. Cothran,[10] D. Crabb,[10] D. Day,[10] J. A. Dunne,[9,§] D. Dutta,[7] R. Ent,[9] B. W. Filippone,[2] A. Honegger,[1] E. W. Hughes,[2] J. Jensen,[2] J. Jourdan,[1] C. E. Keppel,[4,9] D. M. Koltenuk,[8] R. Lindgren,[10] A. Lung,[6,†] D. J. Mack,[9] J. McCarthy,[10] R. D. McKeown,[2] D. Meekins,[11] J. H. Mitchell,[9] H. G. Mkrtchyan,[9] G. Niculescu,[4] I. Niculescu,[4] T. Petitjean,[1] O. Rondon,[10] I. Sick,[1] C. Smith,[10] B. Terburg,[5] W. F. Vulcan,[9] S. A. Wood,[9] C. Yan,[9] J. Zhao,[1] and B. Zihlmann[10]

[1]*University of Basel, Basel, Switzerland*
[2]*Kellogg Radiation Laboratory, California Institute of Technology, Pasadena, California 91125*
[3]*Florida International University, University Park, Florida 33199*
[4]*Hampton University, Hampton, Virginia 23668*
[5]*University of Illinois, Urbana-Champaign, Illinois 61801*
[6]*University of Maryland, College Park, Maryland 20742*
[7]*Northwestern University, Evanston, Illinois 60201*
[8]*University of Pennsylvania, Philadelphia, Pennsylvania 19104*
[9]*Thomas Jefferson National Accelerator Facility, Newport News, Virginia 23606*
[10]*University of Virginia, Charlottesville, Virginia 22901*
[11]*College of William and Mary, Williamsburg, Virginia 23187*

(Received 13 November 1998)

Inclusive electron scattering is measured with 4.045 GeV incident beam energy from C, Fe, and Au targets. The measured energy transfers and angles correspond to a kinematic range for Bjorken $x > 1$ and momentum transfers from $Q^2 = 1-7$ $(\mathrm{GeV}/c)^2$. When analyzed in terms of the y-scaling function the data show for the first time an approach to scaling for values of the initial nucleon momenta significantly greater than the nuclear matter Fermi momentum (i.e., >0.3 GeV/c). [S0031-9007(99)08613-5]

PACS numbers: 25.30.Fj, 13.60.Hb

High energy electron scattering from nuclei can provide important information on the wave function of nucleons in the nucleus. In particular, with simple assumptions about the reaction mechanism, scaling functions can be deduced that, if shown to scale (i.e., are independent of length scale or momentum transfer), can provide information about the momentum and energy distribution of nucleons in a nucleus. Several theoretical studies [1–4] have indicated that such measurements may provide direct access to short-range nucleon-nucleon correlations.

The concept of y scaling in electron-nucleus scattering was first introduced by West [5] and Kawazoe *et al.* [6]. They showed that in the impulse approximation, if quasielastic scattering from a nucleon in the nucleus was the dominant reaction mechanism, a scaling function $F(y)$ could be extracted from the measured cross section which was related to the momentum distribution of the nucleons in the nucleus. In the simplest approximation the corresponding scaling variable y is the minimum momentum of the struck nucleon along the direction of the virtual photon. In general the scaling function depends on both y and momentum transfer—$F(y, Q^2)$—but at sufficiently high Q^2 ($-Q^2$ is the square of the four-momentum transfer) the dependence on Q^2 should vanish yielding scaling. However, the simple impulse approximation picture breaks down when the final-state interactions (FSI) of the struck nucleon with the rest of the nucleus are included. Previous calculations [7–14] suggest that the contributions from final-state interactions should vanish at sufficiently high Q^2. A previous SLAC measurement [15] suggested an approach to the scaling limit for heavy nuclei but only for low values of $|y| < 0.3$ GeV/c at momentum transfers up to 3 $(\mathrm{GeV}/c)^2$. The data presented here represent a significant increase in the Q^2 range compared to previous measurements while also extending the coverage in y.

The present data were obtained in Hall C at the Thomas Jefferson National Accelerator Facility (TJNAF), using 4.045 GeV electron beams with intensities from 10–80 μA. The absolute beam energy was calibrated to 0.08% using 0.8 GeV elastic scattering from carbon and BeO targets and 4.0 GeV elastic scattering from hydrogen. The beam current was monitored with three calibrated resonant cavities. The beam energy resolution was better than 0.05% as defined by the accelerator acceptance. Solid targets of C (2.1% and 5.9% of a radiation length), Fe (1.5% and 5.8% of a radiation length), and Au (5.8% of a radiation length) with natural isotropic abundance were used. Data were also taken with liquid targets of hydrogen and deuterium (nominally 4 and 15 cm in length). Scattering from the hydrogen allows a cross-check of the absolute normalization of the cross section; results from the deuterium target will be presented elsewhere. Less than 1% density variations

 0031-9007/99/82(10)/2056(4)$15.00

were observed for the liquid targets due to beam heating for incident beam currents up to 55 μA (maximum current used for the liquid targets) when the 200 μm $\times$ 200 μm beam was rastered by a pair of electromagnets to the typical spot size of ± 1.2 mm.

The scattered electrons were detected with the high momentum spectrometer (HMS) at angles of 15°, 23°, 30°, 37°, 45°, and 55° and the short orbit spectrometer (SOS) at an angle of 74°. Both spectrometers took data simultaneously with nearly identical detector systems configured for electron detection. Each detector system included two planes of plastic scintillator for triggering, two six-element drift chambers for tracking information, as well as a gas Čerenkov detector and Pb glass calorimeter for particle identification.

The measured tracks were required to reconstruct to the target location. For the HMS, additional cuts were applied to eliminate events produced on the pole pieces of the spectrometer magnets. Cuts were also applied to select electrons and reject π^- using the signals from the Čerenkov detector and calorimeter. The combined efficiency of all the cuts was >98%. The binned events were corrected for spectrometer acceptance using an acceptance function generated by a Monte Carlo calculation [16] that included all apertures within the spectrometer. This calculation accurately reproduced the distributions and cross section from hydrogen elastic scattering. Estimated systematic uncertainties due to the acceptance are <2.5%. Tracking efficiencies were typically 94%–97%. Background from misidentified π^- was negligible for the HMS and <3% in the worst case for the SOS. High energy photons produced principally from π^0 decay can result in secondary electrons following pair production by the photons in the target material. This background, estimated by measuring positron yields with the spectrometer magnetic fields reversed, was negligible for spectrometer angles <55°, but was 3%–10% at 55° and 20%–100% at 74°. The larger values for the contribution of this background are for the 6% radiation length targets and result in an estimated systematic error of 5%–10%. However, because the large backgrounds are present only in kinematic regions where the cross section is very small, the statistical uncertainties dominate the total uncertainty.

Because of the large acceptance of the spectrometers (>6 msr) and the rapid variation of the cross section with θ, there can be a significant variation of the cross section over the acceptance. In order to extract cross sections vs energy transfer ν at fixed scattering angle a bin centering correction must be applied. This is accomplished with a model of the cross section [16] that is constrained to reproduce the angle and energy transfer dependence of the measurements. The cross section model was also used to apply radiative corrections using the iterative technique of Refs. [17,18]. Variations in the form of the model were used to estimate systematic uncertainties in these corrections. The total estimated systematic uncertainties in the bin-centering and radiative corrections were 1%–2% and 2.5%, respectively. Last, a Coulomb correction was applied for the change in the incident and scattered energy due to the Coulomb acceleration from the nuclear charge. This correction was significant ($\sim$10% for Fe and $\sim$20% for Au) for the largest scattering angles of the present experiment.

Figure 1 shows the measured cross sections vs energy loss ν for Fe, where for each angle the Q^2 value at Bjorken $x = Q^2/2M\nu = 1$ is given (this value corresponds to elastic scattering from a free nucleon). Because of the significant smearing due to the Fermi motion and the large contribution from other inelastic processes (e.g., π production, resonance production, and deep inelastic scattering) at these relatively high Q^2, there is little evidence of a quasielastic peak. In fact the sharp bend in the spectrum at $\theta = 15°$ is the only distinctive feature resulting from quasielastic scattering. At larger angles the additional inelastic processes cause even this feature to disappear. It should be noted, however, that quasielastic scattering is still expected to contribute significantly to the cross section for $\nu < Q^2/2M$ ($x > 1$). The minimum measured cross sections were limited by count rate and represent a factor of >100 improvement in sensitivity compared to the previous experiment [15]. This improvement is largely due to the higher beam currents and larger acceptance spectrometers available at TJNAF.

The scaling function is defined as the ratio of the measured cross section to the off-shell electron-nucleon cross section multiplied by a kinematic factor:

$$F(y) = \frac{d^2\sigma}{d\Omega\, d\nu}\,(Z\sigma_p + N\sigma_n)^{-1}\,\frac{q}{[M^2 + (y+q)^2]^{1/2}},$$

where Z and N are, respectively, the number of protons and neutrons in the target nucleus, the off-shell cross sections σ_p and σ_n are taken from σ_{CC1} from Ref. [19] using the elastic form factors from Ref. [20], q is the

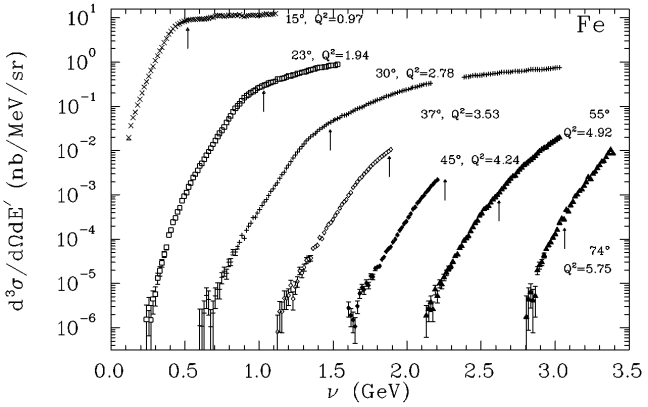

FIG. 1. Differential cross section for Fe. The Q^2 values given at each angle correspond to Bjorken $x = 1$. The value of ν for $x = 1$ is shown by an arrow for each kinematic setting. Statistical errors only are shown.

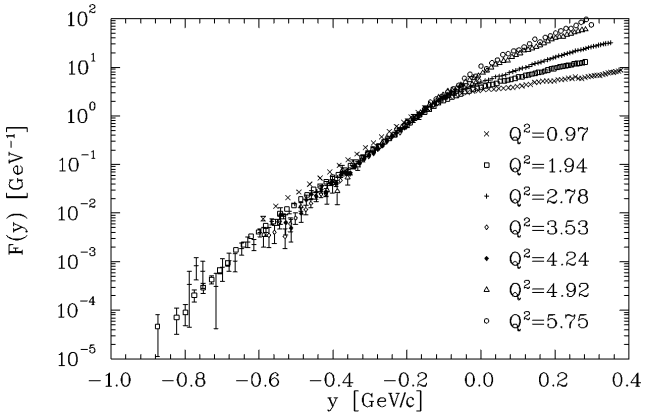

FIG. 2. Scaling function $F(y)$ for Fe. The Q^2 values are given for Bjorken $x = 1$.

three-momentum transfer, and M is the mass of the proton.

The y variable is defined through the equation [21]

$$\nu + M_A = (M^2 + q^2 + y^2 + 2yq)^{1/2} + (M_{A-1}^2 + y^2)^{1/2},$$

where M_A is the mass of the target nucleus and M_{A-1} is the ground state mass of the $A - 1$ nucleus.

The scaling function for Fe is shown in Fig. 2 for all measured angles. While the cross section as a function of Q^2 and ν varies over many orders of magnitude (see Fig. 1), the scaling function for values of $y < -0.1$ GeV/c shows a clear approach to a universal curve where the data can be represented by a function that depends only on y. The breakdown of scaling for values of $y > 0$ is due to the dominance of other inelastic processes beyond quasielastic scattering.

The approach to scaling is also shown in Figs. 3 and 4, where the Q^2 dependence of $F(y)$ at several fixed values of y is presented. For $y = -0.2$ to -0.5 GeV/c there is a clear approach to scaling as Q^2 is increased. This is the first evidence for y scaling in heavy nuclei for $y < -0.3$ GeV/c. There are, in addition, significant scaling violations observed at both low and high Q^2. The increase in $F(y)$ with Q^2 for $y = 0$ and -0.1 GeV/c (Fig. 3) is clearly due to the inelastic processes mentioned above. A similar effect was observed [22] previously, but only for $y \sim 0$. Calculations that include both quasielastic and other inelastic processes [9,14] indicate that at $y = 0$ these other processes dominate the reaction for $Q^2 > 2$ (GeV/c)^2.

At large negative y (Fig. 4) there is a decrease in $F(y)$ with increasing Q^2 as the scaling is approached. This behavior contradicts the approach to scaling expected within the impulse approximation (where the scaling limit is approached from below because of incomplete kinematic coverage at low Q^2) and suggests the influence of final-state interactions. A recent calculation [23] indicates that the component of the FSI resulting from the scattered nucleon interacting with the mean field of the nucleus should be a strongly decreasing function of Q^2 and become negligible for $Q^2 > 3$ (GeV/c)^2. An additional component in the calculation, due to interaction with a correlated nucleon, has a much weaker Q^2 dependence and may persist to the Q^2 range of the present experiment. The present data suggest a scaling that is consistent with an approach to the impulse approximation scaling limit but cannot exclude contributions from FSI that are Q^2 independent.

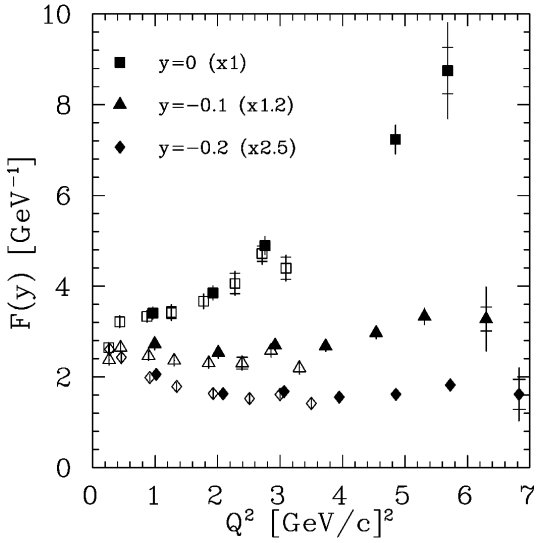

FIG. 3. Scaling function $F(y)$ vs Q^2 for Fe for fixed values of $y = 0$, -0.1, and -0.2 GeV/c. The open points are calculated from the measured cross sections of Ref. [15] including Coulomb corrections and using the definition of y as discussed in the text. The scaling functions for each value of y have been multiplied by the factors in parentheses. The inner error bar is the statistical uncertainty and the outer error bar is the statistical and systematic uncertainty added in quadrature.

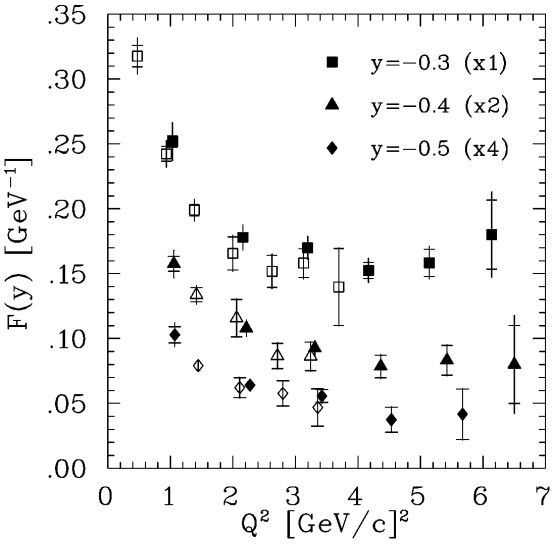

FIG. 4. Same as Fig. 3 for fixed values of $y = -0.3$, -0.4, and -0.5 GeV/c.

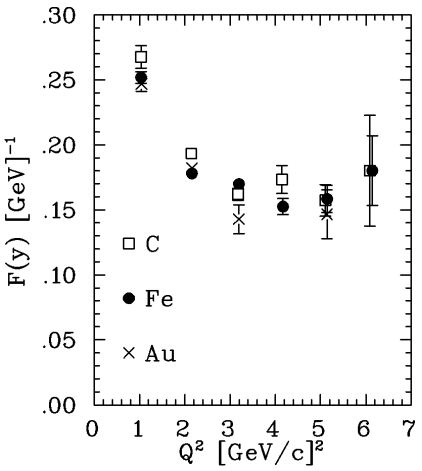

FIG. 5. Scaling function vs Q^2 for C, Fe, and Au at $y = -0.3$ GeV/c. Error bars are statistical only.

Comparison of the scaling functions for C, Fe, and Au show very similar distributions. This can be seen in Fig. 5, where all targets are plotted vs Q^2 for a fixed value of $y = -0.3$ GeV/c. The small A dependence seen in these data is suggestive of a universal response for all medium-mass nuclei as might be expected in a kinematic region dominated by short-range correlations.

The present observation of scaling in a kinematic region expected to be dominated by short-range correlations suggests that inclusive data may be useful in providing experimental constraints on the magnitude of such correlations. Clearly further measurements at higher momentum transfer (e.g., at TJNAF [24]) will be needed to establish the scaling and help identify the role of FSI.

In summary, we have measured the inclusive cross section at $x > 1$ for electrons scattering from C, Fe, and Au targets to $Q^2 \simeq 7$ (GeV/c)^2, a significant increase compared to the previous experiment. When analyzed in terms of the y-scaling function the data show an approach to scaling for $Q^2 > 3$ (GeV/c)^2. At these values of Q^2 a scaling limit can be expected within a simple impulse approximation. In addition a scaling behavior is observed for the first time at very large negative y ($y = -0.5$ GeV/c). This is a regime where the nucleon momentum distribution is expected to be dominated by short-range nucleon-nucleon correlations. It is interesting to note that contributions from short-range final-state interactions may also result in a scalinglike behavior due to the small Q^2 dependence of these effects, and that these contributions are also dominated by short-range nucleon-nucleon correlations.

We gratefully acknowledge the staff and management of TJNAF for their efforts in delivering the electron beam. We also acknowledge helpful discussions with O. Benhar and C. Ciofi degli Atti. This research was supported by the National Science Foundation, the Department of Energy, and the Swiss National Science Foundation.

*Present address: Physics Division, Argonne National Laboratory, Argonne, IL 60439.
†Present address: Thomas Jefferson National Accelerator Facility, Newport News, VA 23606.
‡Present address: College of William and Mary, Williamsburg, VA 23187.
§Present address: Mississippi State University, Mississippi State, MS 39762.

[1] D. Day *et al.*, Annu. Rev. Nucl. Part. Sci. **40**, 357 (1990).
[2] L. L. Frankfurt *et al.*, Phys. Rev. C **48**, 2451 (1993).
[3] C. C. degli Atti and S. Simula, Phys. Lett. B **325**, 276 (1994).
[4] O. Benhar *et al.*, Phys. Lett. B **343**, 47 (1995).
[5] G. B. West, Phys. Rep. **18**, 263 (1975).
[6] Y. Kawazoe, G. Takeda, and H. Matsuzaki, Prog. Theor. Phys. **54**, 1394 (1975).
[7] B. L. Ioffe, V. Khoze, and L. N. Lipatov, *Hard Processes* (North-Holland, Amsterdam, 1984).
[8] E. Pace, G. Salmé, and G. B. West, Phys. Lett. B **273**, 205 (1991).
[9] O. Benhar *et al.*, Phys. Rev. C **44**, 2328 (1991).
[10] O. Greenberg, Phys. Rev. D **47**, 331 (1993).
[11] B. L. Ioffe, JETP Lett. **58**, 930 (1993).
[12] E. Pace, G. Salmé, and A. S. Rinat, Nucl. Phys. **A572**, 1 (1993).
[13] S. A. Gurvitz and A. S. Rinat, Phys. Rev. C **47**, 2901 (1993).
[14] A. S. Rinat and M. F. Taragin, Nucl. Phys. **A620**, 417 (1997); **A624**, 773(E) (1997).
[15] D. B. Day *et al.*, Phys. Rev. Lett. **59**, 427 (1987).
[16] J. Arrington, Ph.D. thesis, California Institute of Technology: www.krl.caltech.edu/~johna/thesis, 1998.
[17] S. Stein *et al.*, Phys. Rev. D **12**, 1884 (1975).
[18] D. H. Potterveld, Ph.D. thesis, California Institute of Technology, 1989.
[19] T. DeForest, Nucl. Phys. **A392**, 232 (1983).
[20] M. Gari and W. Krümpelmann, Phys. Lett. **141B**, 295 (1984).
[21] E. Pace and G. Salmé, Phys. Lett. **110B**, 411 (1982).
[22] J. Arrington *et al.*, Phys. Rev. C **53**, 2248 (1996).
[23] S. Simula (private communication).
[24] TJNAF proposal 99-015, spokespersons A. Lung, D. Day, and B. Filippone, 1999.